


## Article

# The Influence of Burst-Firing EMF on Forskolin-Induced Pheochromocytoma (PC12) Plasma Membrane Extensions

Trevor N. Carniello <sup>1,2,3,\*</sup>, Robert M. Lafrenie <sup>1,2,3</sup>  and Blake T. Dotta <sup>1,2,3</sup>

<sup>1</sup> Department of Biology, Laurentian University, Sudbury, ON P3E 2C6, Canada; rlafrenie@laurentian.ca (R.M.L.); bx\_dotta@laurentian.ca (B.T.D.)

<sup>2</sup> Behavioural Neuroscience Program, Laurentian University, Sudbury, ON P3E 2C6, Canada

<sup>3</sup> Biomolecular Sciences Program, Laurentian University, Sudbury, ON P3E 2C6, Canada

\* Correspondence: tn\_carniello@laurentian.ca

**Abstract:** Previous research has demonstrated that pheochromocytoma (PC12) cells treated with forskolin provides a model for the in vitro examination of neuritogenesis. Exposure to electromagnetic fields (EMFs), especially those which have been designed to mimic biological function, can influence the functions of various biological systems. We aimed to assess whether exposure of PC12 cells treated with forskolin to patterned EMF would produce more plasma membrane extensions (PME) as compared to PC12 cells treated with forskolin alone (i.e., no EMF exposure). In addition, we aimed to determine whether the differences observed between the proportion of PME of PC12 cells treated with forskolin and exposed to EMF were specific to the intensity, pattern, or timing of the applied EMF. Our results showed an overall increase in PME for PC12 cells treated with forskolin and exposed to Burst-firing EMF as compared to PC12 cells receiving forskolin alone. No other patterned EMF investigated were deemed to be effective. Furthermore, intensity and timing of the Burst-firing pattern did not significantly alter the proportion of PME of PC12 cells treated with forskolin and exposed to patterned EMF.

**Keywords:** pheochromocytoma (PC12) cells; electromagnetic fields (EMF); Burst-firing EMF; forskolin; plasma membrane extensions (PME)



**Citation:** Carniello, T.N.; Lafrenie, R.M.; Dotta, B.T. The Influence of Burst-Firing EMF on Forskolin-Induced Pheochromocytoma (PC12) Plasma Membrane Extensions. *NeuroSci* **2021**, *2*, 383–399. <https://doi.org/10.3390/neurosci2040028>

Academic Editor:  
Giuseppina Martella

Received: 12 October 2021  
Accepted: 3 November 2021  
Published: 6 November 2021

**Publisher's Note:** MDPI stays neutral with regard to jurisdictional claims in published maps and institutional affiliations.



**Copyright:** © 2021 by the authors. Licensee MDPI, Basel, Switzerland. This article is an open access article distributed under the terms and conditions of the Creative Commons Attribution (CC BY) license (<https://creativecommons.org/licenses/by/4.0/>).

## 1. Introduction

Pheochromocytoma (PC12) cells can be induced to produce plasma membrane extensions that have been previously characterized to exhibit morphological and physiological features similar to those of peripheral neurons [1–4]. Differentiated PC12 cells are electrically excitable and are capable of producing and secreting classical neurotransmitters, such as dopamine and serotonin [5,6]. Having inducible morphological and physiological features make PC12 cells an excellent model to investigate the mechanisms of neurogenesis and neuronal activity. Treating PC12 cells with various neurotrophic factors, such as NGF, has been shown to promote survival and differentiation as measured by the production of plasma membrane extensions typified as neuronal projections [7–10]. The promotion of neuritic projections involves activation of biomolecular cascades involving cyclic adenosine monophosphate (cAMP), protein kinase A (PKA), and extracellular regulated kinase (ERK) [11–15]. Treatment of PC12 cells with forskolin, a diterpene that can promote activation of cAMP levels, has been shown to reliably produce neuron-like projections [7–9,16–20]. Recently, Zhang et al. [21] showed that, under appropriate conditions, applications of specific wavelengths of light (electromagnetic radiation) could enhance neurite extensions in PC12 cells in the absence of chemical stimulation, thus circumventing the need for physio-chemical factors to promote differentiation in this cell line. Based on Zhang and colleagues [21] findings, it was hypothesized that different forms of electromagnetic radiation (e.g., weak, patterned electromagnetic fields) may also promote or neurite outgrowth.

Our lab has previously shown that exposures to specific time-varying, physiologically patterned, propagating electromagnetic fields (EMF) can affect biological systems [22–30]. For example, exposure to a frequency-modulated EMF called the Thomas-EMF is capable of reducing proliferation of B16-BL6 melanoma cells *in vivo* and *in vitro* [31–33]. This same patterned EMF (e.g., the Thomas-EMF) was also shown to increase analgesia (reduce nociceptive responses) in rats and affect the growth rates of bisected planaria and cancer cells [28,34–39]. Our lab has also shown that exposure to an EMF based on the firing pattern of amygdaloid neurons (Burst-firing EMF) [40–43] was capable of inducing analgesia in rats [44], ameliorated self-reported mood and depression scores in human participants [45,46], and activated mu opioid receptors in cancer cells without enhancing their growth [28]. The possibility that PC12 cell neurite outgrowth may be affected by appropriately patterned EMF exposure warrants investigation.

There were several aims to the investigations outlined in this article. Our prime objective was to determine whether PC12 cells treated with the combination of forskolin and exposed to patterned EMF showed significantly different proportions of plasma membrane extensions (PME) as compared to PC12 cells treated with forskolin only. A second goal for these investigations was to determine whether enhancements in the proportion of PME of PC12 cells treated with forskolin and exposed to weak, time-varying EMF was pattern specific or non-specific. Finally, if enhancements in PME of PC12 cells treated with forskolin and exposed to weak, time-varying EMF is pattern specific, we aimed to determine what additional effects, if any, may be observed when the EMF parameters (e.g., timing, intensity) are modulated.

## 2. Methods

### 2.1. Cell Culture and Induction of Plasma Membrane Extensions

Pheochromocytoma (PC12) cells (ATCC, Rockville, MD, USA), derived from the rat adrenal medulla, were grown to confluence on 100 mm stock plates in RPMI-1640 media supplemented with 10% horse serum, 5% fetal bovine serum (Hyclone, Fisher Scientific, Mississauga, ON, USA), and 1% antibiotic and antimycotic at 37 °C in a humidified incubator with 5% CO<sub>2</sub>. For all experiments, 50 µL of the cell suspension (approximately 20,000 cells) in complete media were allowed to adhere to poly-L-lysine-treated, 35 mm cell culture dishes for 24 h at 37 °C. The media were then replaced with 2 mL of serum-free RPMI-1640 media and the cells were exposed to the indicated EMF pattern or sham conditions in and treated with 0.5 µM forskolin at ten minutes during exposure. Forskolin treatment facilitated the initiation (priming) and induction of PC12 cells neurite extensions.

Plating densities ranged from  $1.20 \times 10^4$  to  $6.41 \times 10^4$  cell/cm<sup>2</sup> per 35-mm dish. These plating densities fall within the “low” category of plating density as reported by other researchers in the field. PC12 cells have a tendency to form clusters or clump together at higher densities [13,47]. Maintaining a low plating density minimizes the possibility of clumping which may underestimate the number of extensions attributed to chemical treatment (i.e., forskolin) and EMF exposure.

### 2.2. Exposure Apparatus

The EMF-generating device consisted of a 12 × 12 × 12 cm cube of Plexiglass. Each side of the Plexiglass cube was fitted with a reed relay solenoid (5VDC Reed Relay, 0.5A at 125VAC; Radio Shack, Sault Ste. Marie, MI; #275-232). Solenoids from opposing faces were wired in a manner so as to allow opposing pairs and all three pairs to be operated independently or simultaneously in any combination. The device, named the 4D box by its developer, was designed in a way as to allow generated EMFs to be presented through all three geometric planes in any combination [32,33]. Photos corresponding to the 4-D application geometry can be found in Figure A1.

The 4-D exposure device (i.e., EMF-generating device) was controlled by a custom constructed digital-to-analog converter (DAC). The DAC served to convert digital computer code to voltage equivalents with an output range between –5 and +5 V, and was outfitted

with a variable resistor able to adjust the resultant EMF intensity. The digital code for any patterned EMF generated through the 4-D box consisted of a series of integer values ranging from 0–256. The DAC was designed in a way that values between 0–126 of the electromagnetic field (EMF) pattern were translated to negative voltage (e.g., 0 = –5 V), while a value of 127 within the patterned EMF code produces 0 V, and values between 128–256 of patterned EMF code produce positive voltage (e.g., 256 = +5 V). A custom computer software program was developed to upload and run various patterned EMFs typically employed by this laboratory. The software program allowed the experimenter to set the point-duration, inter-stimulus interval, total exposure duration, and the combination of which pairs of solenoids the EMF will be generated from. For all experiments described in this document, point-duration (PD) refers to the amount of time current presented to the EMF-generating device for each of the points of the digital code that makes up the EMF pattern. The inter-stimulus interval (ISI) refers to the delay between successive pattern presentations throughout the exposure duration.

### 2.3. Exposure Protocols

All experiments were conducted in a tissue culture laboratory located on the 7th floor of Laurentian University's Science II building. The tissue culture lab contained two identical, standard tissue culture incubators. One incubator was devoted to maintaining stock cultures of PC12 cells and the other was devoted to experimental investigations, primarily EMF exposures. Exposure and stock culture incubators were maintained at  $37 \pm 0.1$  °C and  $5 \pm 0.2\%$  CO<sub>2</sub>. Experimental plates were prepared according to the methods discussed in Section 2.1. On any experimental day, a sham and active EMF exposure trial was conducted. The order of exposure was counter-balanced across trials. All sham and active EMF exposures were conducted in the exposure incubator and all replicates were completed on separate days. The presence (or lack thereof) of the experimental EMF was verified using a mini-audio amplifier coupled to a magnetic telephone pick-up, while intensity was verified using an AC milliGauss meter (AlphaLabs). Unless otherwise specified, each experimental condition was conducted on two plates of PC12 cells and replicated in triplicate. A photo of the standard exposure set-up can be found in Figure A2. For comparisons, sham exposures (i.e., patterned EMF is not present) serve as control conditions. We reiterate the purpose of these investigations was to determine whether the combination of patterned EMF and forskolin produced a greater proportion of PME as compared to forskolin alone.

### 2.4. Experiment #1—Exposure to Burst-Firing EMF for 1 and 3 h

The primary goal for this experiment was to determine whether the combination of exposure to Burst-firing EMF and forskolin improved the proportion of PME as compared to forskolin alone. The second directive was to determine whether longer EMF exposure durations (3 h) improved the proportion of PME as compared to shorter (1 h) exposures. Thus, for this experiment, prepared pheochromocytoma (PC12) cells were exposed to either Sham or Burst-firing EMF generated through the 4-D exposure apparatus for 1 and 3 h. The Burst-firing EMF was generated by converting a series of 230 points, ranging from 0 to 256, to voltage equivalents. A diagrammatic representation of the Burst-firing EMF configuration can be found in Figure A3. In this experiment, the Burst-firing pattern (PD = 3 msec, ISI = 3 msec; Intensity = 2–4 μT) was applied through opposing pairs of solenoids and was rotated along all three spatial axes for 500 msec followed by the simultaneous activation of all 6 solenoids for 500 msec. Sham exposures consisted of placing the PC12 cells in the EMF-generating device and with the device off. The only manipulation Sham exposures received was the injection of forskolin at 10 min into the procedure. Length of exposure to Sham and Burst-firing EMF condition were 1 and 3 h.

### 2.5. Experiment #2—Exposure to Different Patterned EMF

The aim of Experiment #2 was to determine whether differences observed between PC12 cells treated with the combination of forskolin and exposed to patterned EMFs and PC12 cells receiving only forskolin (i.e., sham conditions) were specific to the pattern of the applied EMF or non-specific. To this end, we compared the combination of forskolin-treated PC12 cells exposed to Burst-firing EMF to cells treated with forskolin alone (Sham) and PC12 cells treated with forskolin and exposed to one of three other EMF patterns: Reverse Burst-firing, Thomas-EMF, and 7-Hz pulse. The 7-Hz pulse consisted of a 690-msec 7-Hz sine wave followed by a 210 msec pause. The reverse Burst-firing pattern consisted of the same series of 230 points which made up the Burst-firing pattern, however the series of integers were inverted. The Thomas-EMF was generated by converting 859 integer values between 0 and 256 to a corresponding voltage of  $-5$  V to  $+5$  V ( $127 = 0$  V). The series of points composing the Thomas-EMF produced 18 doublet peaks with gradually increasing intervals between 3 msec (for the first 5 repeats) to 120 msec for the last 5 repeats. The resulting frequency modulation for the Thomas-EMF pattern ranged from 25 Hz for the first 5 to 6 Hz for the last 5 repeats. For a more detailed description of the Thomas-EMF see Buckner et al., 2015 and Buckner, Buckner, Koren, Persinger, & Lafrenie 2018. Pictures of the Burst-firing, reverse Burst, Thomas-EMF, and 7-Hz pulse patterns can be found in Figure A4. For all patterned EMF applications, PD and ISI were set to 3 msec and peak intensities were set between 2 and 4  $\mu$ T. For each trial, two plates were conducted in parallel, four photos were sampled from each plate for analysis, and all trials were independently replicated three times.

### 2.6. Experiment #3—Identifying the Influence of Burst-Firing EMF Timing on PC12 PME

The aim of Experiment #3 was to determine whether there is an optimal timing to the Burst-firing EMF that will enhance the proportion of PME when PC12 cells are exposed to the combination of forskolin and patterned EMF as compared to forskolin alone. Here, we compared 3 different combinations of PD and ISI: (1) PD = 1 msec, ISI = 2 msec, (2) PD = 3 msec, ISI = 3 msec, and (3) PD = 3 msec, ISI = 3000 msec for the Burst-firing pattern. All 3 EMF exposure conditions lasted 1 h and were combined with forskolin treatment. Comparisons were made in reference to PC12 cells that only received forskolin treatment.

### 2.7. Experiment #4—Investigating the Role of Intensity of Burst-Firing EMF on PC12 Cell PME

The aim of this experiment was to determine whether PC12 cells treated with forskolin and exposed to varying intensities of the Burst-firing EMF would result in differences in the proportion of PME as compared to PC12 cells treated with forskolin only (i.e., Sham). In this experiment, plates of PC12 cells treated with forskolin were exposed to the Burst-firing EMF (PD = 3 msec, ISI = 3 msec) at one of three intensities: (1) 300–500 nT (low), (2) 3–5  $\mu$ T (medium) and (3)  $>10$   $\mu$ T (high). Intensities were verified using an AC milliGauss meter (AlphaLabs) and exposures lasted 1 h.

### 2.8. Experiment #5—Examining Differences in the Proportion of PC12 PME between Changing and Constant EMF Exposure

Experiment 5 was designed to investigate whether there were any differences in the proportion of PME between changing and constant EMF exposures. Rather than focus on differences between the combination of forskolin and EMF applications to PC12 cells treated with forskolin alone, this experiment aimed to determine differences between EMF applications only. There were two exposure conditions: (1) changing EMF and (2) constant EMF. In the “constant” EMF exposure group, PC12 cells treated with forskolin were exposed to the Burst-firing EMF (PD = 3 msec, ISI = 3 msec; Intensity 3–5  $\mu$ T) generated through all 6 solenoids of the 4-D exposure apparatus for 1 h. In the “changing” EMF condition, the Burst-firing EMF (PD = 3 msec, ISI = 3 msec; Intensity 3–5  $\mu$ T) was generated through opposing pairs of solenoids for the duration of 500 msec and rotated across all 3 spatial axes at the same interval, before all 6 solenoids were activated simultaneously for 500 msec.

To elaborate, considering the surface of the cell dish to be in the X-plane, the dish would be exposed first to the Burst-firing EMF from the pair of solenoids in the parallel plane for 500 msec, followed by the pair of solenoids in perpendicular plane for 500 msec, then the Burst-firing EMF would be presented by the pair of solenoids in the orthogonal plane for 500 msec, before being presented through all 6 solenoids (3 pairs) simultaneously for 500 msec. The rotated pattern (parallel, perpendicular, orthogonal, all) would be repeated throughout the 1 h exposure duration.

### 2.9. Cell Morphological Measures

To assess the morphology of the cells, 4 photos of each plate were taken 3 days after receiving the EMF exposure using a phase-contrast microscope at 100× magnification. The total number of cells were counted for each image and the number of cells bearing plasma membrane extensions were counted and reported as a proportion of the total cell count. Criteria to be counted as a PME were set such that the microscopist was able to visually discern a qualitatively distinct protrusion or extension that could be traced back to the cell soma. We were not interested in quantitative measures such as the length of the extension, as we were aiming to examine robust effects that could be appreciated by less experienced microscopists and observable under these conditions. Additional measures included: the proportion of cells with multipolar and higher order arborisations, the number of inter-cellular connections (i.e., synapses), and the proportion of cells whose plasma membrane extensions exceeded the diameter of the cell soma at its largest extent. Again, the threshold criteria for additional morphological measures, under each classification, was such that the microscopist could easily discern qualitatively distinct features. There was no difference in any of the measures for cells exposed to EMF for 1 h versus 3 h and so data were reported only for 1 h exposures. Similarly, there was no difference in the morphology of the cells measured at 3 days versus 6 days after exposure and so data are reported only for images obtained 3 days after exposure.

### 2.10. Statistical Methods

Raw data for morphological measures were converted into a proportion (percent) of the total cells counted (feature of interest/total cell count × 100%) and were used in subsequent analyses. Unless otherwise specified, all proportions were subjected to a one-way analysis of variance. Subsequent Tukey's post-hoc tests, where applicable, were employed to demonstrate which source(s) of variance were driving the effect. All analyses were conducted using SPSS version 23 and data were considered significant at the  $p < 0.05$  level. Bonferroni alpha-wise correction was applied to accommodate alpha-level error of multiple tests.

## 3. Results

### 3.1. Descriptive Statistics

Average cell count per field of view, average number of pheochromocytoma (PC12) cells bearing plasma-membrane extensions (PME) per field of view, and computed total cell density (cells/cm<sup>2</sup>) and PME density average over the samples corresponding to each investigation are summarized in Table 1. For convenience, any sham condition represents exposures where PC12 only received forskolin treatment (i.e., control conditions), while any experimental condition that PC12 cells are exposed to an electromagnetic field (EMF) reflects the combination of forskolin and the target EMF pattern.

**Table 1.** The average of the total number of cells counted per field of view, at a magnification of 100×, average number of PC12 cells bearing plasma membrane extensions (PME), and the computed cell and PME density across each experiment and exposure condition within the experiment. As mentioned previously, sham exposures (control) are PC12 cells treated with forskolin only and all other EMF conditions are samples of PC12 cells treated with both forskolin and exposed to an EMF. For the cell total and PME columns, means and SEM (in brackets) are reported. Measures of density are reported in terms of number of cells/cm<sup>2</sup>. Number of samples refers to the total number of plates exposed to a given condition. In each experiment, 2 plates were exposed in tandem, 4 photos were sampled from each plate for assessment of cell morphology, and a minimum of 3 replications were completed for each condition within a given experiment.

Experiment	Condition	Average Cell Total	Number of Replicates	Total Number of Plates Sampled	Average Cell Density (Cells/cm <sup>2</sup> )	Average PME	Average PME Density (Cells/cm <sup>2</sup> )
Experiment #1 Exposure Duration	Sham 1 h	628.5 (175.64)	3	6	$4.76 \times 10^4$	105.5 (32.35)	$7.99 \times 10^3$
	Sham 3 h	613.00 (180.92)	3	6	$4.64 \times 10^4$	101.33 (28.98)	$7.67 \times 10^3$
	Burst 1 h	421.5 (160.82)	3	6	$3.19 \times 10^4$	113.67 (47.92)	$8.61 \times 10^3$
	Burst 3 h	392.17 (166.22)	3	6	$2.97 \times 10^4$	103.77 (42.36)	$7.86 \times 10^3$
Experiment #2 Rotation vs. Constant	Rotation	163.94 (57.96)	4	8	$1.24 \times 10^4$	71.75 (20.61)	$5.43 \times 10^3$
	Constant	222.13 (60.31)	4	8	$1.68 \times 10^4$	68.00 (22.06)	$5.13 \times 10^3$
Experiment #3 Point Duration	Sham	594.75 (78.30)	12	24	$4.50 \times 10^4$	107.00 (14.79)	$8.10 \times 10^3$
	Burst (3,3)	348.5 (132.73)	3	6	$2.64 \times 10^4$	107.17 (33.26)	$8.11 \times 10^3$
	Burst (1,1)	298.33 (166.64)	3	6	$2.26 \times 10^4$	91.83 (49.61)	$6.96 \times 10^3$
	Burst (33,000)	159.00 (23.39)	3	6	$1.20 \times 10^4$	53.83 (7.61)	$4.08 \times 10^3$
Experiment #4 Intensity	Sham	690.75 (112.35)	6	12	$5.23 \times 10^4$	119.54 (21.98)	$9.06 \times 10^3$
	Low	465.17 (27.16)	3	6	$3.52 \times 10^4$	120.50 (10.83)	$9.13 \times 10^3$
	Med	314.5 (89.31)	3	6	$2.38 \times 10^4$	85.17 (26.87)	$6.45 \times 10^3$
	Hi	310.67 (43.25)	3	6	$2.35 \times 10^4$	88.00 (4.49)	$6.67 \times 10^3$
Experiment #5 EMF Pattern	Sham	594.75 (78.30)	12	24	$4.51 \times 10^4$	107.42 (14.79)	$8.14 \times 10^3$
	Thomas	846.17 (166.88)	3	6	$6.41 \times 10^4$	52.03 (21.24)	$3.94 \times 10^3$
	Burst	212.67 (54.73)	3	6	$1.61 \times 10^4$	47.00 (10.89)	$3.26 \times 10^3$
	Rev-Burst	251.17 (57.28)	3	6	$1.90 \times 10^4$	33.33 (7.07)	$2.53 \times 10^3$
	7-Hz	304.84 (81.01)	3	6	$2.31 \times 10^4$	63.29 (25.84)	$4.79 \times 10^3$

Results of Experiment #1–Exposure to spatially-rotated, Burst-firing EMF on induced PC12 plasma membrane extensions: PC12 cells treated with 0.5 μM forskolin and exposed to a spatially-rotated Burst-firing EMF for 1 and 3 h showed a significantly greater proportion of PME compared to cells exposed to sham conditions 3 and 6 days following treatment (Figure 1). Results of a one-way analysis of variance revealed significant differences for the proportion of PME-bearing cells on Day 3 [ $F_{(1,26)} = 6.48, p = 0.017, \Omega^2\text{-est} = 0.21$ ] and Day 6 [ $F_{(1,26)} = 7.24, p = 0.013, \Omega^2\text{-est} = 0.22$ ] between exposure condition (sham versus field) with no difference across days.

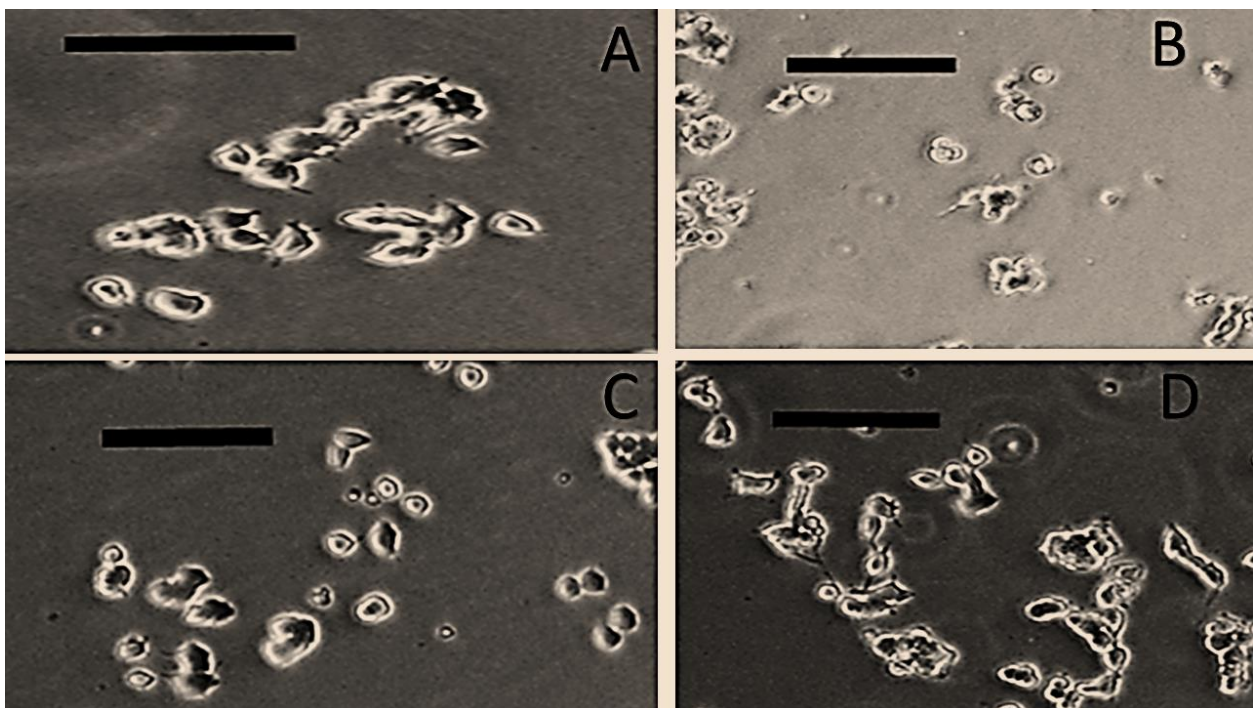
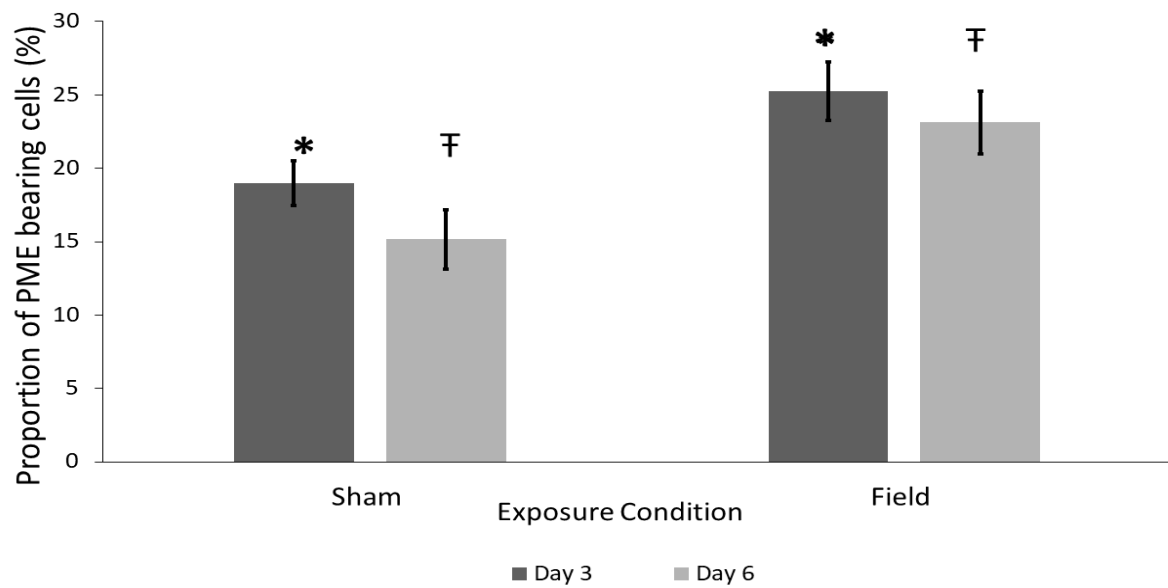


**Figure 1.** PC12 cells were exposed to the Burst-firing EMF pattern (PD = 3 msec, ISI = 3 msec; peak intensity 40 mG) generated by the 4-D application geometry with 2-Hz spatial rotation across all three axes, treated with 0.5  $\mu$ M of forskolin and the proportion of PME-bearing cells determined. Sham treatments serve as the control condition (forskolin only). The graph (upper panel) represents the proportion of PC12 cells bearing PME following the 1-h Burst-firing EMF or Sham exposures. Error bars represent SEM. \* and F indicate significant differences between conditions ( $p < 0.05$ ). Supporting photos show representative samples comparing 1 h exposures to the Sham condition measured (A) 3 days and (B) 6 days after exposure and 1 h exposures to Burst-firing EMF measured (C) 3 days and (D) 6 days after exposure. Dark bars were fitted to original photos prior to their magnification and adjustment. Darkened bars measure approximately 100  $\mu$ m in length for each individual photo. For each condition there were 2 plates conducted in parallel, 4 sample photos assessed per plate, and all trials were repeated in triplicate.

### 3.2. Results of Experiment #5—Determining the Difference between Rotational or Constant Application of Burst-Firing EMF Generated through the 4-D Exposure Application

PC12 cells treated with 0.5  $\mu\text{M}$  forskolin and exposed to a spatially-rotating Burst-firing EMF showed the same proportion of PME as cells treated with the same concentration of forskolin and exposed to a constant application of Burst-firing EMF. One-way analysis of variance showed that spatio-temporal presentation (constant versus rotated applications) did not significantly affect the proportion of cells bearing PME ( $p > 0.05$ ) or any other morphological measure between treatment conditions ( $p > 0.05$ ; Figure 2).

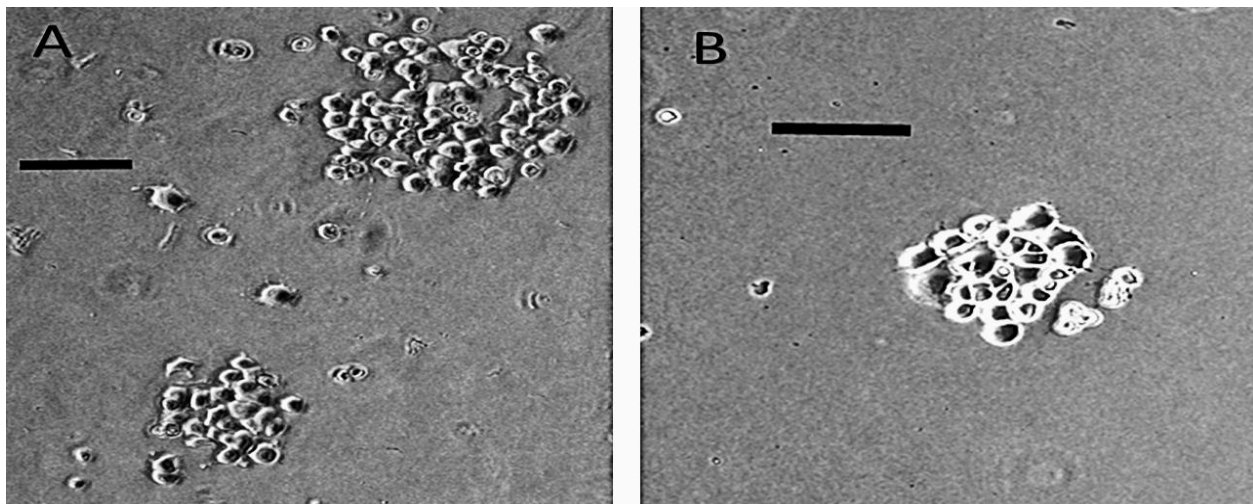
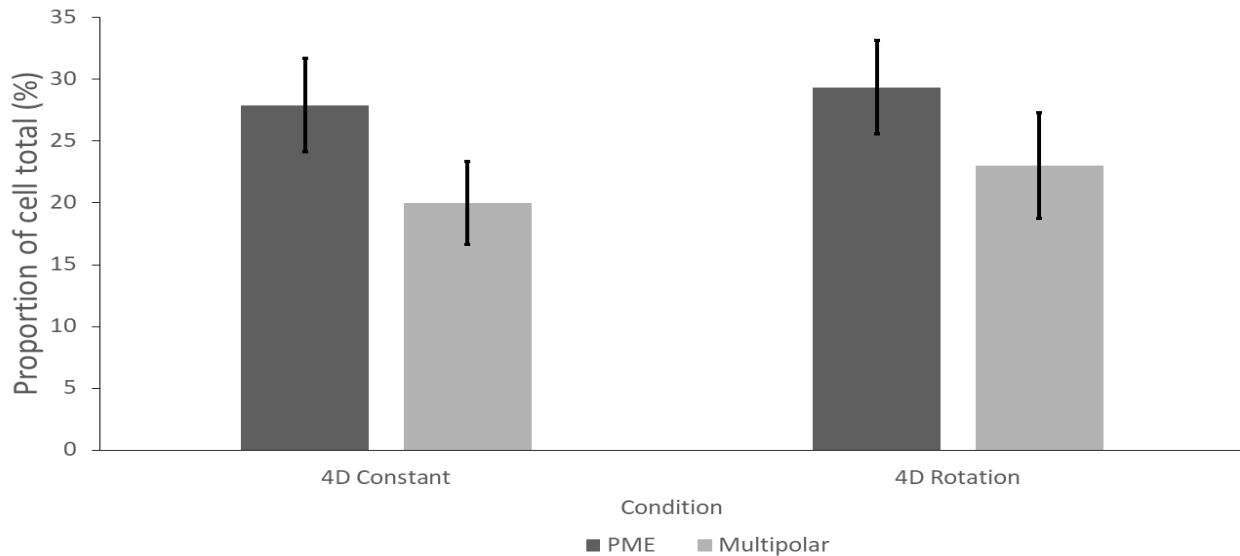


**Figure 2.** PC12 cells were exposed to Burst-firing EMF in the 4-D box as a function of spatio-temporal pattern of presentation (constant versus rotated) and the proportion of PME determined and compared. The graph (upper panel) demonstrates differences in the proportion of PME (dark bar) and multipolar extensions (light bar) across EMF exposure conditions. Error bars in the graph represent SEM. For each condition (constant and rotation), each trial was conducted in triplicate, 2 plates were conducted in parallel, and 4 samples per plate were photographed for cell counts in each condition. Both the constant and rotated exposures were conducted on PC12 cells that were treated with 0.5  $\mu\text{M}$  of forskolin. Supporting photos show representative images of cells exposed to the constant (A; left) and rotated (B; right) 1 h, Burst-firing EMF. Darkened bars were fitted to original photos prior to their adjustment. Each darkened bar approximates 100  $\mu\text{m}$  in length for the individual photo for which they have been fitted.



### 3.3. Results of Experiment #3—The Influence of Point Duration of Burst-Firing EMF on PC12 Plasma Membrane Extensions

PC12 cells treated with 0.5  $\mu\text{M}$  forskolin and exposed to 1-h Burst-firing EMF showed increased proportion of PME, independent of changes in PD and ISI timing (Figure 3). One-way analysis of variance revealed significant differences for the proportion of PME-bearing [ $F_{(3,35)} = 5.83, p = 0.003, \Omega^2\text{-est} = 0.35$ ] and multipolar cells [ $F_{(3,35)} = 8.27, p = 3.24 \times 10^{-4}, \Omega^2\text{-est} = 0.44$ ] between Burst-firing EMF treated samples and Sham exposures. There was no difference between any of the different combinations of PD and ISI used in this investigation.

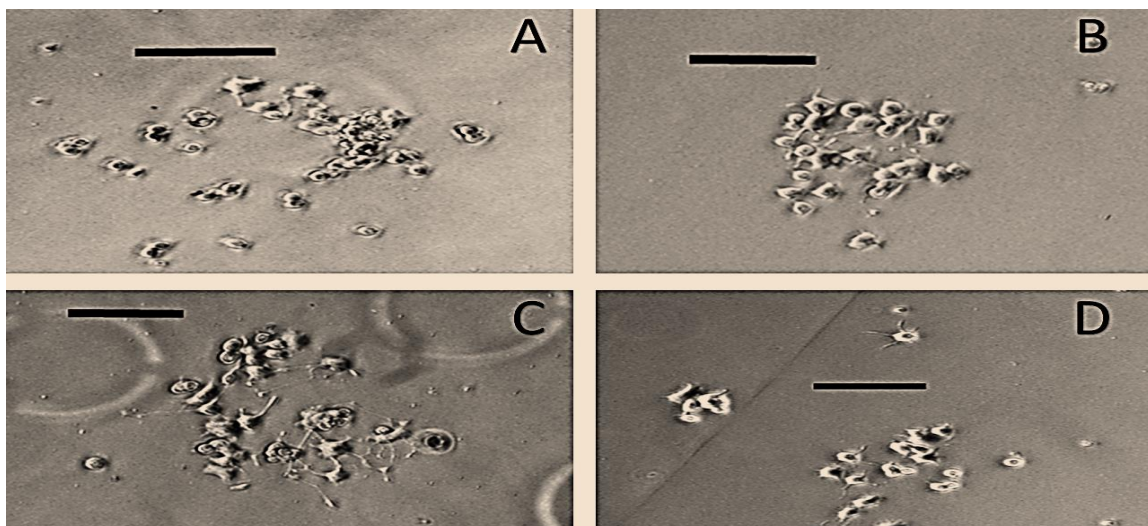
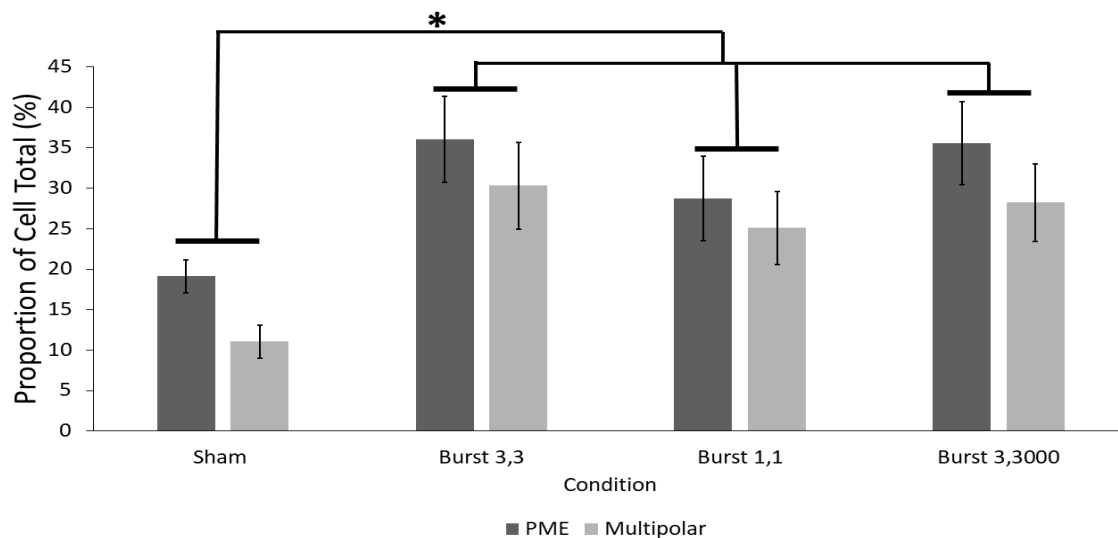


**Figure 3.** The graph (upper panel) shows the the proportion of PC12 cells expressing PME (dark bar) and multipolar extensions (light bar) as a function of exposure to different PD and ISI settings for the Burst-firing EMF. Error bars represent SEM. \* indicates significant differences between groups ( $p < 0.05$ ). The photo shows representative samples of PC12 cells 3 days after exposure to (A): 1 h Sham exposures; (B), Burst-firing EMF with PD: 3 msec, ISI: 3 msec; (C), Burst-firing EMF with PD: 1 msec, ISI: 1 msec; and, (D), Burst-firing EMF with PD: 3 msec, ISI: 3000 msec. Darkened bars were fitted to original microscope photos and adjusted for clarity. Individual darkened bars approximate 100  $\mu\text{m}$  in length. As discussed previously, sham treatments are PC12 cells treated with forskolin only, while all EMF exposures were treatments where cells received both forskolin treatment and EMF. For each exposure condition, 2 plates were conducted in parallel within a given trial, 4 photos were sampled from each plate for cell counting in a given trial, and all trials were triplicated for each condition. Sham conditions were replicated 12 times; each Sham exposure consisted of 2 plates conducted simultaneously and 4 photos were sampled from each plate to assess cell morphology.

The efficacy of the pattern of EMF application on the proportion of plasma membrane extensions in PC12 cells treated with sub-micromolar ( $0.5 \mu\text{M}$ ) concentrations of forskolin was tested.

### 3.4. Results of Experiment #4—Effect of Intensity of Burst-Firing EMF on Plasma Membrane Extensions in PC12 Cultures

Different intensities of Burst-firing EMF did not change the proportion of PME in PC12 cells treated with  $0.5 \mu\text{M}$  forskolin and exposed to EMF (Figure 4). A one-way analysis of variance revealed statistically significant differences in the proportion of PME-bearing cells [ $F(2,29) = 6.08, p = 0.003, \Omega^2\text{-est} = 0.41$ ] and multipolar cells [ $F(3,29) = 12.36, p = 3.3 \times 10^{-5}, \Omega^2\text{-est} = 0.59$ ] which was shown to be driven by the significantly lower proportions of PME in Sham-treated cells by Tukey's post-hoc analysis. No differences were obtained between the highest intensity and all other EMF exposure intensities.

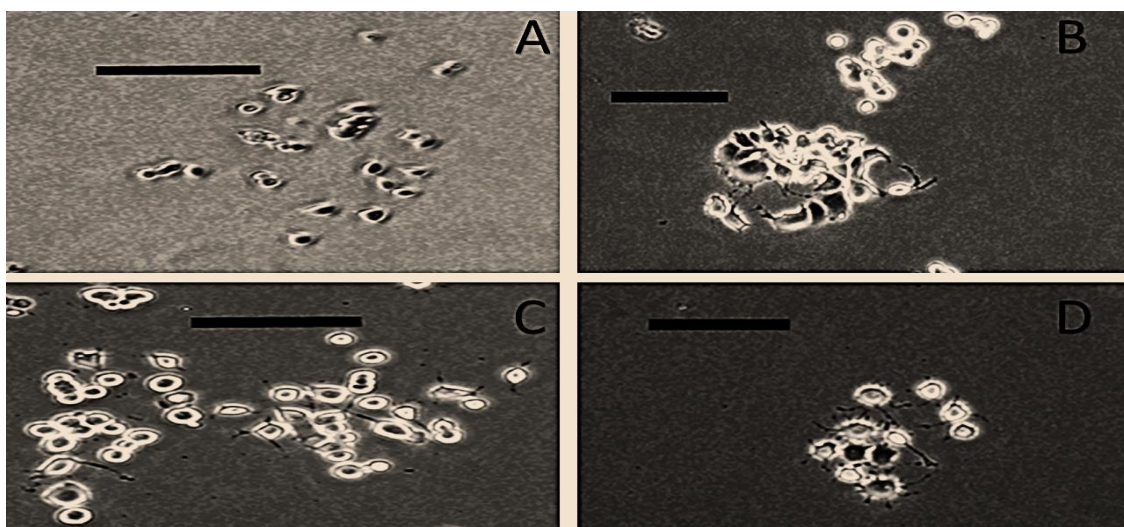
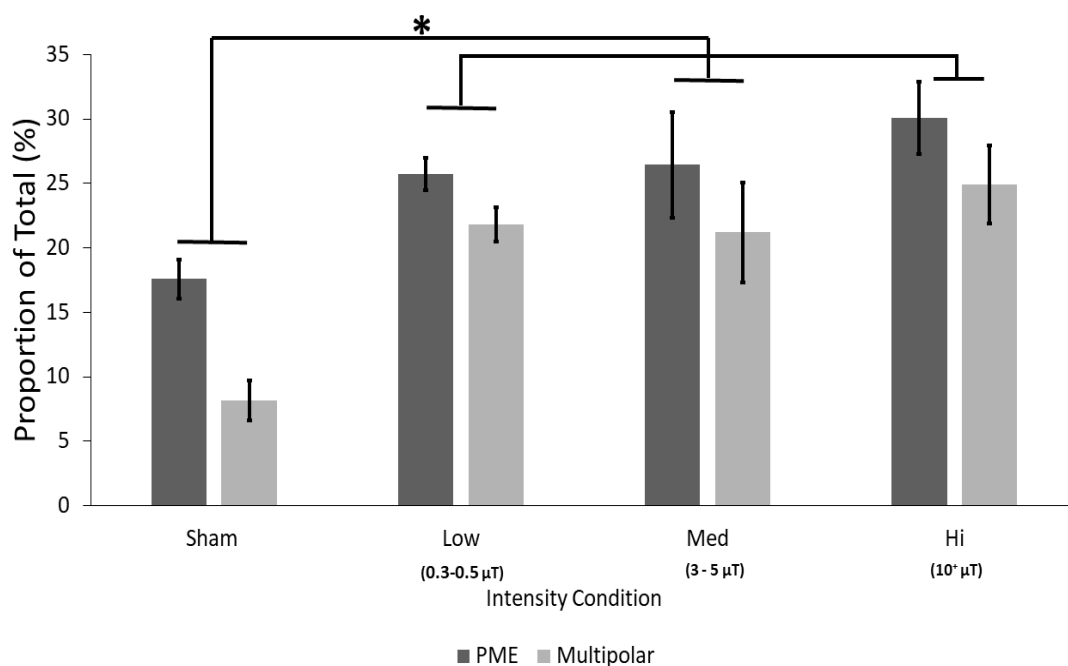


**Figure 4.** The graph (upper panel) shows the differences in the proportion of PME-bearing (dark bar) and multipolar extensions (light bar) of PC12 cells treated with the combination of  $0.5 \mu\text{M}$  of forskolin and exposed to 1-h Burst-firing EMF

of different intensities. Error bars represent SEM. Sham conditions were replicated 6 times and all other conditions were replicated in triplicate. For each replication, 2 plates were exposed in parallel and 4 sample photos were taken from each plate for cell counting. \* indicates significant differences between groups ( $p < 0.05$ ). The photo shows representative images of PC12 cells exposed for 1 h to: (A). Sham conditions; (B), low intensity (0.3–0.5  $\mu\text{T}$ ); (C), medium intensity (3–5  $\mu\text{T}$ ); and, (D), high intensity ( $10^+$   $\mu\text{T}$ ) Burst-firing EMF. Darkened bars were fitted to original microscope photos and adjusted for clarity. Individual darkened bars approximate 100  $\mu\text{m}$  in length. Recall that sham treatments are PC12 cells treated with forskolin only (control), while all EMF exposures were treatments where cells received both forskolin treatment and EMF.

### 3.5. Results of Experiment # 2—Pattern Specificity of EMF Application on Forskolin Induced PC12 Plasma Membrane Extensions

PC12 cells treated with 0.5  $\mu\text{M}$  forskolin and exposed to EMF showed different effects on PME depending on the particular patterned EMF (Figure 5). Analyses of variance indicated significant differences between the proportion of PME-bearing [ $F_{(4,29)} = 3.93$ ,  $p = 0.031$ ,  $\Omega^2\text{-est} = 0.39$ ] and multipolar cells [ $F_{(4,29)} = 4.71$ ,  $p = 0.006$ ,  $\Omega^2\text{-est} = 0.43$ ] as a function of patterned EMF exposure. Tukey's post-hoc tests showed that the proportion of PME and multipolar extensions in the Burst-firing EMF and 7-Hz pulse EMF conditions were significantly greater than Sham condition, Thomas-EMF, and Reverse-Burst-firing EMF conditions which were not different from each other.

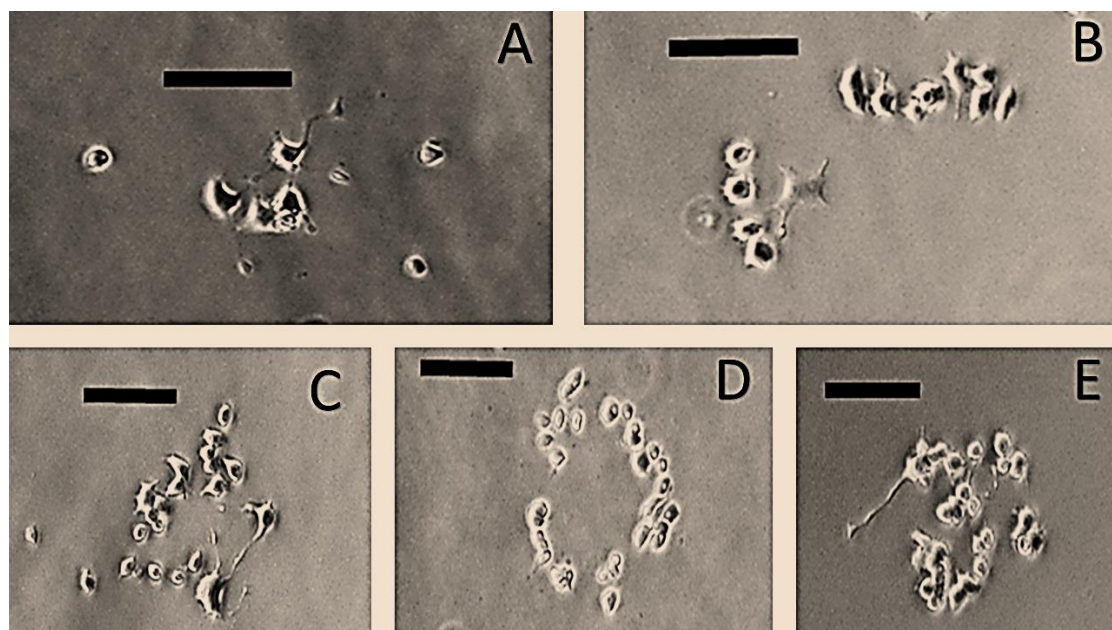
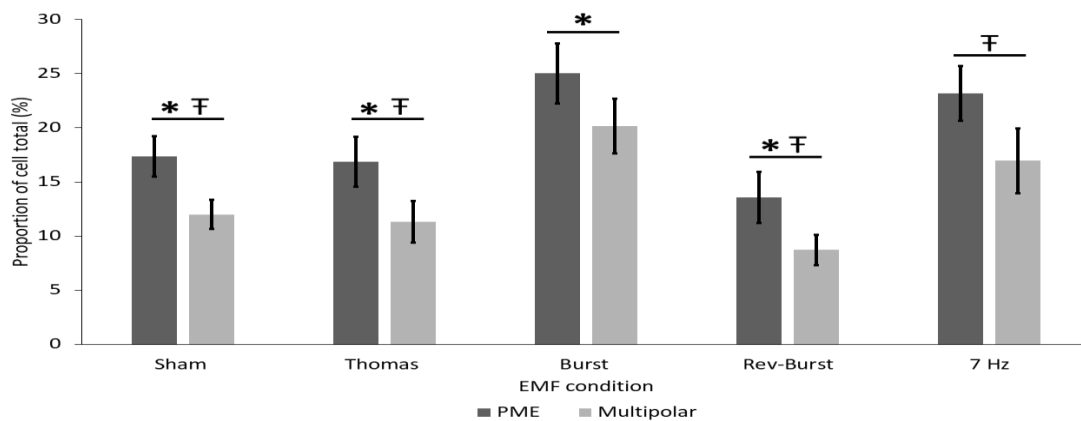


**Figure 5.** The graph (upper panel) shows differences in morphology between PC12 cells treated with 0.5  $\mu\text{M}$  forskolin and exposed to different patterned EMF with PD and ISI set to 3 msec and verified intensity within 2–4  $\mu\text{T}$  for 1 h. The proportion of

cell total for plasma membrane extensions (PME) are represented in the dark bars, whilst the proportion of the multipolar cells are represented in the light bars. Error bars correspond to SEMs. For each exposure condition, 2 plates were conducted in parallel for a given replicate, 4 sample photos were taken from each plate for cell counting, and all conditions were replicated 3 times. \* and † identify significant differences between experimental groups ( $p < 0.05$ ). The photo shows representative images from PC12 cells exposed to: (A), Sham conditions; (B), Thomas-EMF; (C), Burst-firing EMF; (D), Reverse burst-firing EMF; and, (E), 7-Hz pulse EMF. Darkened bars were fitted to original microscope photos and adjusted for clarity. Individual darkened bars approximate 100  $\mu\text{m}$  in length. As noted previously, sham treatments are PC12 cells treated with forskolin only (control), while all EMF exposures were treatments where cells received both forskolin treatment and EMF.

#### 4. Discussion

In this study we showed that exposure to a particular EMF pattern, Burst-firing EMF, could promote neuritogenesis in PC12 cells treated with suboptimal levels of forskolin, a cAMP activator, when compared to PC12 cells that received forskolin alone. There are several inferences derived from the results of the outlined experiments. Firstly, the exposure of PC12 cells to Burst-firing EMF in combination with forskolin increased the proportion of PME as compared to PC12 cells treated with forskolin alone. Secondly, there were no differences in the proportion of PME between shorter (1 h) and longer (3 h) exposures to the Burst-firing EMF; however, the proportions of PME in both 1 and 3-h Burst-firing EMF conditions were significantly greater than the proportion of PME of PC12 cells treated with forskolin alone. Thirdly, there were no differences between groups of PC12 cells treated with forskolin and exposed to different timings of the Burst-firing EMF; however, all timing groups had a significantly greater proportion of PME as compared to forskolin-only conditions. Fourthly, similar findings were observed when examining different intensities of the Burst-firing EMF; there were no differences in the proportion of PME between the different EMF intensities, however all intensities tested had a significantly greater proportion of PME as compared to PC12 cells treated with forskolin alone. Lastly, the combined treatment of forskolin and exposure to either Burst-firing EMF or 7-Hz pulsed EMF was able to produce a significantly greater proportion of PME as compared to PC12 cells treated with forskolin alone or the combination of forskolin and exposure to Reverse Burst-firing EMF and Thomas-EMF.

Most notably, our results indicated that PC12 cells treated with 0.5  $\mu\text{M}$  forskolin and exposed to Burst-firing EMF presented though pairs of solenoids arranged across the 3 spatial axes enhanced neurite formation as measured by the proportion of treated cells that expressed PME or multipolar extensions as compared to PC12 cells treated with forskolin alone. The results of these studies show that there is a specificity of the applied EMF pattern in order to appreciably alter the proportion of observed PME as compared to chemical only treatment. For example, exposure to the Burst-firing EMF was the most successful at increasing the proportion of PME-bearing cells and the proportion of cells with multipolar extensions. Exposure to the Thomas-EMF and the Reverse-Burst-EMF did not affect PC12 morphology. The observation that the inverted presentation of the Burst-firing EMF, reverse-Burst, was no longer able to promote neuritogenesis suggests that simply supplying the same energy to the system is not sufficient to affect PC12 cells under these conditions but the pattern of the EMF is critical in mediating its effects. Exposure to the 7-Hz pulse was also able to increase the proportion of PME-bearing cells, similar to the Burst-firing pattern.

PC12 cells that are induced to differentiate by treatment with neurotrophic factors become responsive to dopamine and are similar to peripheral dopaminergic neurons [48–50]. Exposure to the Burst-firing pattern has been shown to act, at least partially, on  $\mu$ -opioid receptors [28], which are related to the biomolecular features of dopamine reactions [51–53]. The 7-Hz pulse has some similarity to naturally occurring electromagnetic fluctuations in the environment such as the geomagnetic field (that which arises from the rotation of Earth's fluid iron core) and Schumann harmonics (the consequence of lightning discharges between the Earth's surface and the ionosphere). Exposure to this frequency has remarkable impacts on animal behaviour and neurodevelopment [54–56]. Although unsubstantiated,

it is possible that the 7-Hz pulse activates neuritogenesis in the PC12 model by mimicking fluctuations in the geomagnetic field, although more rigorous experimental investigations are warranted.

The spatial presentation of the Burst-firing EMF also did not seem to be critical in mediating effects on PC12 neuritogenesis. Exposure to rotated presentations of the Burst-firing EMF through the three spatial axes did not show any difference in PC12 cell PME from exposure to constant presentation through all 3 pairs of solenoids simultaneously. In this case, the pattern of the EMF is not different (i.e., same content) and therefore presentation in both the rotated and constant conditions are argued to provide appropriate stimulation to elicit the observed effects. Exposure to Burst-firing EMF appears to be able to affect PC12 neuritogenesis over a wide range of intensities. PC12 cells exposed to Burst-firing EMF at low intensity (300–500 nT), medium intensity (3–5  $\mu$ T) or high intensity ( $10^+$   $\mu$ T) were all able to increase the proportion of cells expressing PME or multipolar extensions to a similar level than exposure to sham conditions. One interpretation of this result is that there is a threshold of intensity required to affect the PC12 cell morphology and any stimulus greater than that intensity is effective. Again, limitations arise as the technology employed does not allow the field strengths to exceed 15  $\mu$ T and it is possible that higher intensities may render differing results.

Data collected comparing the 1 and 3-h exposure durations to the Burst-firing EMF revealed no statistical differences in the proportion of PME-bearing cells between these two exposure conditions. The simplest explanation for this observation is that the 1 h exposure is sufficient to activate the required signal transduction pathway to induce PME in PC12 cells and that both the 1 and 3 h exposures are spontaneously downregulated with similar kinetics. For these experiments, a suboptimal concentration of forskolin, which can induce cAMP production, is required for the exposure to Burst-firing EMF to induce PME; it was previously shown that exposure to Burst-firing EMF alone is unable to induce PME. This suggests that Burst-firing EMF and forskolin work in a synergistic manner. This would indicate that forskolin and Burst-firing EMF work via different but complementary signalling pathways. One candidate pathway to explain the effect of Burst-firing EMF is the MEK/ERK pathway. Maintained activation of the MEK/ERK pathway is quintessential to the formation of PME as evidenced by results of studies using nerve growth factor [9,14,27]. Further, exposure to other physiologically patterned EMF has been shown to promote activation of the MEK/ERK pathway [33]. Additional experiments to address this possibility are required.

We conclude that the effects of EMF application on PC12 cells treated with forskolin are contingent upon the pattern of the applied field. Different intensities of the exposure or discrete changes in the temporal construction of the pattern (i.e., timing) were all still able to promote the changes in PC12 morphology. However, exposure to the inverted configuration of the Burst-firing field in combination with forskolin was not able to alter PC12 morphology.

**Author Contributions:** Conceptualization, T.N.C.; methodology, T.N.C. and R.M.L.; formal analysis, T.N.C. and B.T.D.; investigation, T.N.C.; data curation, T.N.C., R.M.L. and B.T.D.; writing—original draft preparation, T.N.C., R.M.L. and B.T.D.; writing—review and editing, T.N.C. All authors have read and agreed to the published version of the manuscript.

**Funding:** This research received no external funding.

**Institutional Review Board Statement:** Not applicable.

**Informed Consent Statement:** Not applicable.

**Data Availability Statement:** The data presented in this study are available on request from the corresponding author.

**Conflicts of Interest:** The authors declare no conflict of interest.

## Appendix A

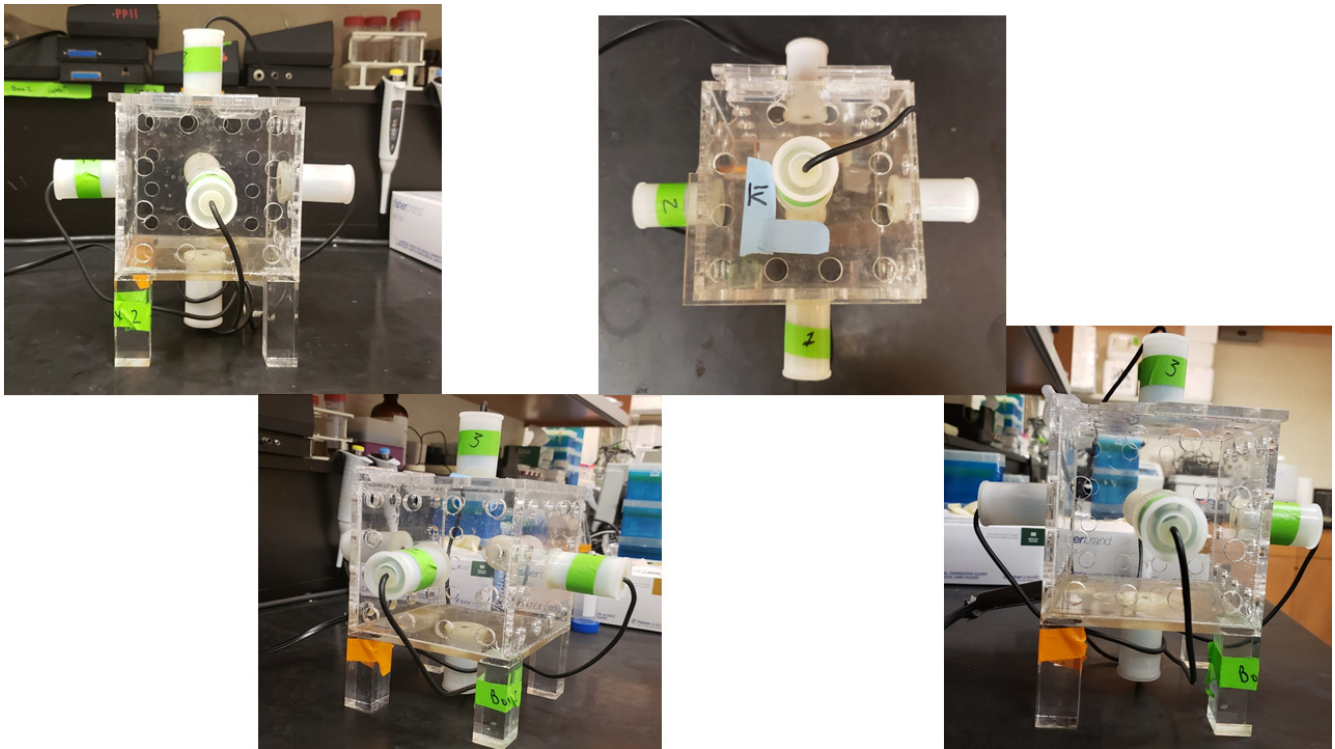


**Figure A1.** Photographic representation of the 4-D exposure apparatus from different points of view. Front (top left); Top (Top right), Corner (bottom left), side (bottom right).



**Figure A2.** Photographic representation of the 4-D application geometry with corresponding computer generated patterned EMF (computer) and custom built digital-to-analog converter (DAC; blue box).

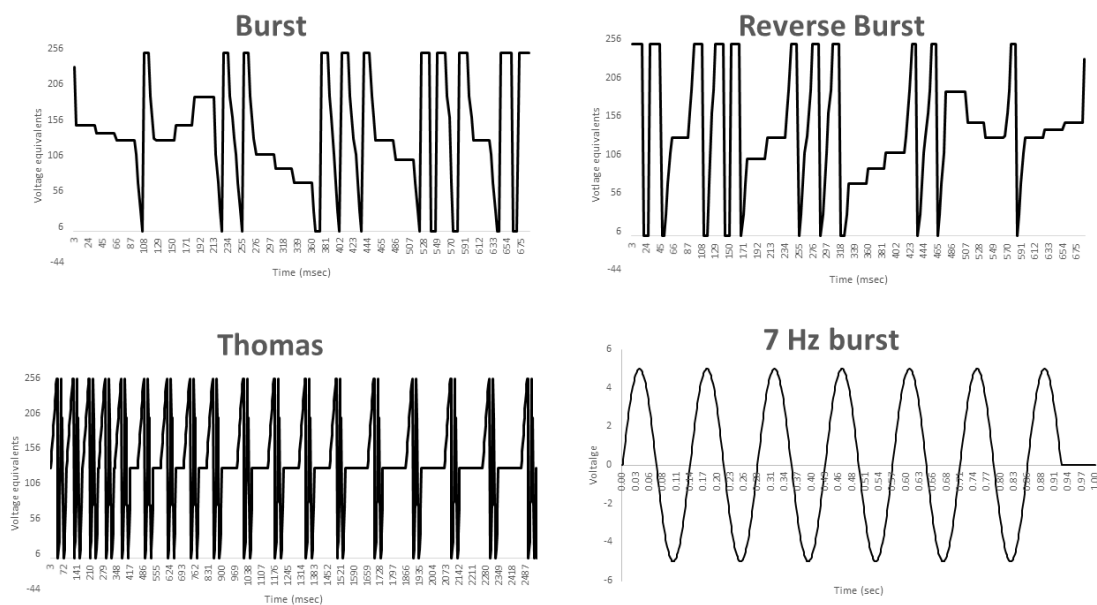


**Figure A3.** Graphical representation of the burst-firing EMF pattern.

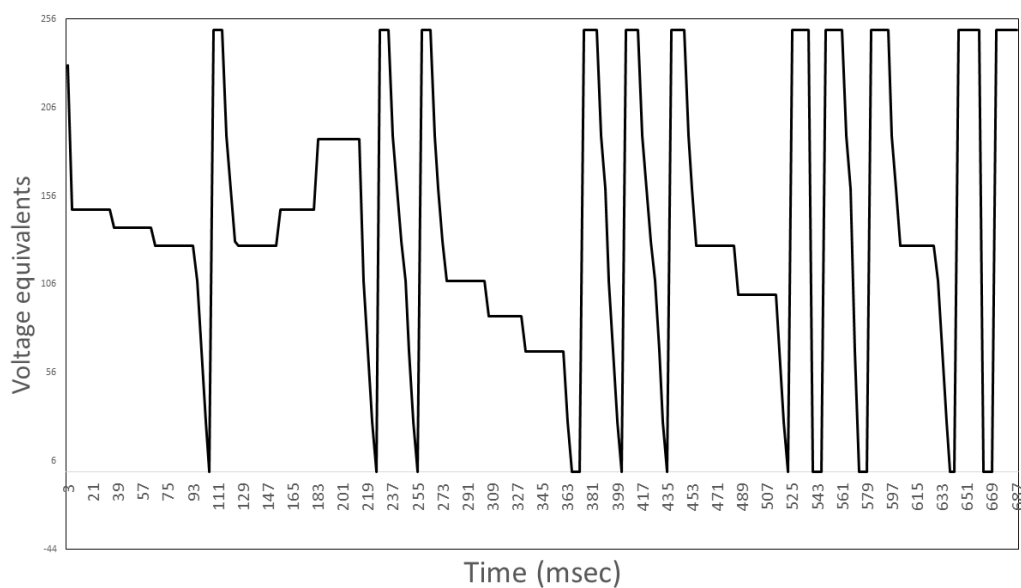


**Figure A4.** Graphical representation of the burst-firing (top left), reverse burst firing (top right), Thomas (bottom left), and 7-Hz burst (bottom right) patterns.

## References

- Greene, L.A.; Tischler, A.S. PC12 Pheochromocytoma Cultures in Neurobiological Research. In *Advances in Cellular Neurobiology*; Elsevier: Amsterdam, The Netherlands, 1982; Volume 3, pp. 373–414.
- Greene, L.A.; Tischler, A. Establishment of a noradrenergic clonal line of rat adrenal pheochromocytoma cells which respond to nerve growth factor. *Proc. Natl. Acad. Sci. USA* **1976**, *73*, 2424–2428. [[CrossRef](#)] [[PubMed](#)]
- Tischler, A.S.; Greene, L. Morphologic and cytochemical properties of a clonal line of rat adrenal pheochromocytoma cells which respond to nerve growth factor. *Lab. Invest.* **1978**, *39*, 77–89.
- Tischler, A.; Greene, L.; Kwan, P.; Slayton, V. Ultrastructural effects of nerve growth factor on PC 12 pheochromocytoma cells in spinner culture. *Cell Tissue Res.* **1983**, *228*, 641–648. [[CrossRef](#)] [[PubMed](#)]
- Satpute, R.; Hariharakrishnan, J.; Bhattacharya, R. Effect of alpha-ketoglutarate and N-acetyl cysteine on cyanide-induced oxidative stress mediated cell death in PC12 cells. *Toxicol. Ind. Heal.* **2010**, *26*, 297–308. [[CrossRef](#)]
- Shafer, T.; Atchison, W.D. Transmitter, ion channel and receptor properties of pheochromocytoma (PC12) cells: A model for neurotoxicological studies. *NeuroToxicology* **1991**, *12*, 473–492. [[PubMed](#)]
- Caillaud, T.; Opstal, W.Y.X.-V.; Scarcériaux, V.; Billardon, C.; Rostène, W. Treatment of PC12 cells by nerve growth factor, dexamethasone, and forskolin. *Mol. Neurobiol.* **1995**, *10*, 105–114. [[CrossRef](#)] [[PubMed](#)]

8. Gunning, P.W.; E Landreth, G.; A Bothwell, M.; Shooter, E.M. Differential and synergistic actions of nerve growth factor and cyclic AMP in PC12 cells. *J. Cell Biol.* **1981**, *89*, 240–245. [[CrossRef](#)]
9. Loeb, D.M.; Maragos, J.; Martin-Zanca, D.; Chao, M.; Parada, L.F.; Greene, L.A. The trk proto-oncogene rescues NGF responsiveness in mutant NGF-nonresponsive PC12 cell lines. *Cell* **1991**, *66*, 961–966. [[CrossRef](#)]
10. Vaudry, D.; Stork, P.J.S.; Lazarovici, P.; Eiden, L.E. Signaling Pathways for PC12 Cell Differentiation: Making the Right Connections. *Science* **2002**, *296*, 1648–1649. [[CrossRef](#)] [[PubMed](#)]
11. Bos, J.; De Bruyn, K.; Enserink, J.; Kuiperij, B.; Rangarajan, S.; Rehmann, H.; Riedl, J.; De Rooij, J.; Van Mansfeld, F.; Zwartkruis, F. The role of Rap1 in integrin-mediated cell adhesion. *Biochem. Soc. Trans.* **2003**, *31*, 83–86. [[CrossRef](#)]
12. Greene, L.A.; McGuire, J.C. Induction of ornithine decarboxylase by nerve growth factor dissociated from effects on survival and neurite outgrowth. *Nat. Cell Biol.* **1978**, *276*, 191–194. [[CrossRef](#)] [[PubMed](#)]
13. Park, K.H.; Park, H.J.; Shin, K.S.; Choi, H.S.; Kai, M.; Lee, M.K. Modulation of PC12 Cell Viability by Forskolin-Induced Cyclic AMP Levels Through ERK and JNK Pathways: An Implication for L-DOPA-Induced Cytotoxicity in Nigrostriatal Dopamine Neurons. *Toxicol. Sci.* **2012**, *128*, 247–257. [[CrossRef](#)]
14. York, R.D.; Yao, H.; Dillon, T.; Ellig, C.L.; Eckert, S.P.; McCleskey, E.W.; Stork, P.J.S. Rap1 mediates sustained MAP kinase activation induced by nerve growth factor. *Nat. Cell Biol.* **1998**, *392*, 622–626. [[CrossRef](#)]
15. Wang, Z.; Dillon, T.J.; Pokala, V.; Mishra, S.; Labudda, K.; Hunter, B.; Stork, P.J.S. Rap1-Mediated Activation of Extracellular Signal-Regulated Kinases by Cyclic AMP Is Dependent on the Mode of Rap1 Activation. *Mol. Cell. Biol.* **2006**, *26*, 2130–2145. [[CrossRef](#)]
16. Park, T.; Kim, K.-T. Cyclic AMP-Independent Inhibition of Voltage-Sensitive Calcium Channels by Forskolin in PC12 Cells. *J. Neurochem.* **2002**, *66*, 83–88. [[CrossRef](#)] [[PubMed](#)]
17. Richter-Landsberg, C.; Jastorff, B. The role of cAMP in nerve growth factor-promoted neurite outgrowth in PC12 cells. *J. Cell Biol.* **1986**, *102*, 821–829. [[CrossRef](#)]
18. Seamon, K.B.; Daly, J.W. Forskolin: A unique diterpene activator of cyclic AMP-generating systems. *J. Cycl. Nucleotide Res.* **1981**, *7*, 201–224.
19. Seamon, K.B.; Daly, J.W. Forskolin, cyclic AMP and cellular physiology. *Trends Pharmacol. Sci.* **1983**, *4*, 120–123. [[CrossRef](#)]
20. Seamon, K.B.; Padgett, W.; Daly, J.W. Forskolin: Unique diterpene activator of adenylate cyclase in membranes and in intact cells. *Proc. Natl. Acad. Sci. USA* **1981**, *78*, 3363–3367. [[CrossRef](#)]
21. Zhang, K.; Duan, L.; Ong, Q.; Lin, Z.; Varman, P.M.; Sung, K.; Cui, B. Light-Mediated Kinetic Control Reveals the Temporal Effect of the Raf/MEK/ERK Pathway in PC12 Cell Neurite Outgrowth. *PLoS ONE* **2014**, *9*, e92917. [[CrossRef](#)]
22. Cook, C.M.; Persinger, M.A. Experimental Induction of the “Sensed Presence” in Normal Subjects and an Exceptional Subject. *Percept. Mot. Ski.* **1997**, *85*, 683–693. [[CrossRef](#)]
23. Karbowski, L.M.; Harribance, S.L.; Buckner, C.A.; Mulligan, B.P.; Koren, S.A.; Lafrenie, R.M.; Persinger, M.A. Digitized quantitative electroencephalographic patterns applied as magnetic fields inhibit melanoma cell proliferation in culture. *Neurosci. Lett.* **2012**, *523*, 131–134. [[CrossRef](#)]
24. Mach, Q.H.; Persinger, M.A. Behavioral changes with brief exposures to weak magnetic fields patterned to stimulate long-term potentiation. *Brain Res.* **2009**, *1261*, 45–53. [[CrossRef](#)]
25. Meli, S.C.; Persinger, M.A. Red Light Facilitates the Sensed Presence Elicited by Application of Weak, Burst-Firing Magnetic Fields Over the Temporal Lobes. *Int. J. Neurosci.* **2009**, *119*, 68–75. [[CrossRef](#)] [[PubMed](#)]
26. Murugan, N.J.; Karbowski, L.M.; Lafrenie, R.; Persinger, M.A. Maintained Exposure to Spring Water but Not Double Distilled Water in Darkness and Thixotropic Conditions to Weak (~1 μT) Temporally Patterned Magnetic Fields Shift Photon Spectroscopic Wavelengths: Effects of Different Shielding Materials. *J. Biophys. Chem.* **2015**, *6*, 14–28. [[CrossRef](#)]
27. Murugan, N.J.; Karbowski, L.M.; Persinger, M.A. Serial pH increments (~20 to 40 milliseconds) in water during exposures to weak, physiologically patterned magnetic fields: Implications for consciousness. *Water* **2014**, *6*, 45–60.
28. Murugan, N.J.; Karbowski, L.M.; Persinger, M.A. Weak Burst-firing magnetic fields that produce analgesia equivalent to morphine do not initiate activation of proliferation pathways in human breast cells in culture. *Integr. Cancer Sci. Ther.* **2014**, *1*, 47–50.
29. Ross, M.L.; Koren, S.A.; Persinger, M.A. Physiologically Patterned Weak Magnetic Fields Applied Over Left Frontal Lobe Increase Acceptance of False Statements as True. *Electromagn. Biol. Med.* **2008**, *27*, 365–371. [[CrossRef](#)] [[PubMed](#)]
30. Whissell, P.D.; Persinger, M.A. Emerging synergisms between drugs and physiologically-patterned weak magnetic fields: Implications for neuropharmacology and the human population in the twenty-first century. *Curr. Neuropharmacol.* **2007**, *5*, 278–288. [[CrossRef](#)]
31. Buckner, C.A.; Buckner, A.L.; Koren, S.A.; Persinger, M.A.; Lafrenie, R.M. Inhibition of Cancer Cell Growth by Exposure to a Specific Time-Varying Electromagnetic Field Involves T-Type Calcium Channels. *PLoS ONE* **2015**, *10*, e0124136. [[CrossRef](#)]
32. Buckner, C.A.; Buckner, A.L.; Koren, S.A.; Persinger, M.A.; Lafrenie, R.M. The effects of electromagnetic fields on B16-BL6 cells are dependent on their spatial and temporal character. *Bioelectromagnetics* **2017**, *38*, 165–174. [[CrossRef](#)]
33. Buckner, C.A.; Buckner, A.L.; Koren, S.A.; Persinger, M.A.; Lafrenie, R.M. Exposure to a specific time-varying electromagnetic field inhibits cell proliferation via cAMP and ERK signaling in cancer cells. *Bioelectromagnetics* **2018**, *39*, 217–230. [[CrossRef](#)]
34. Dotta, B.T.; Buckner, C.A.; Lafrenie, R.M.; Persinger, M.A. Photon emissions from human brain and cell culture exposed to distally rotating magnetic fields shared by separate light-stimulated brains and cells. *Brain Res.* **2011**, *1388*, 77–88. [[CrossRef](#)]



35. Dotta, B.T.; Lafrenie, R.M.; Karbowski, L.M.; Persinger, M.A. Photon emission from melanoma cells during brief stimulation by patterned magnetic fields: Is the source coupled to rotational diffusion within the membrane? *Gen. Physiol. Biophys.* **2014**, *33*, 63–73. [[CrossRef](#)]
36. Dotta, B.T.; Murugan, N.J.; Karbowski, L.M.; Koren, S.A. Rotational Frequency Matching of the Energy of the Changing Angular Velocity Magnetic Field Intensity and the Proton Magnetic Moment Produces a Ten Fold Increased Excess Correlation in pH Shifts in Spring Water. *NeuroQuantology* **2015**, *14*. [[CrossRef](#)]
37. Dotta, B.T.; Persinger, M.A. “Doubling” of local photon emissions when two simultaneous, spatially-separated, chemiluminescent reactions share the same magnetic field configurations. *J. Biophys. Chem.* **2012**, *03*, 72–80. [[CrossRef](#)]
38. Murugan, N.J.; Karbowski, L.M.; Lafrenie, R.M.; Persinger, M.A. Temporally-Patterned Magnetic Fields Induce Complete Fragmentation in Planaria. *PLoS ONE* **2013**, *8*, e61714. [[CrossRef](#)] [[PubMed](#)]
39. Tessaro, L.W.; Persinger, M.A. Optimal durations of single exposures to a frequency-modulated magnetic field immediately after bisection in planarian predict final growth values. *Bioelectromagnetics* **2013**, *34*, 613–617. [[CrossRef](#)] [[PubMed](#)]
40. Martin, L.; Koren, S.A.; Persinger, M.A. Thermal Analgesic Effects from Weak, Complex Magnetic Fields: Critical Parameters. *Electromagn. Biol. Med.* **2005**, *24*, 65–85. [[CrossRef](#)]
41. Martin, L.; Persinger, M.A. Spatial Heterogeneity Not Homogeneity of the Magnetic Field during Exposures to Complex Frequency-Modulated Patterns Facilitates Analgesia. *Percept. Mot. Ski.* **2003**, *96*, 1005–1012. [[CrossRef](#)] [[PubMed](#)]
42. Martin, L.; Persinger, M. Thermal analgesia induced by 30-min exposure to 1  $\mu$ T burst-firing magnetic fields is strongly enhanced in a dose-dependent manner by the  $\alpha$ 2 agonist clonidine in rats. *Neurosci. Lett.* **2004**, *366*, 226–229. [[CrossRef](#)] [[PubMed](#)]
43. Martin, L.; Persinger, M.A. The Influence of Various Pharmacological Agents on the Analgesia Induced by an Applied Complex Magnetic Field Treatment: A Receptor System Potpourri. *Electromagn. Biol. Med.* **2005**, *24*, 87–97. [[CrossRef](#)]
44. Fleming, J.L.; Persinger, M.A.; Koren, S.A. Magnetic Pulses Elevate Nociceptive Thresholds: Comparisons with Opiate Receptor Compounds in Normal and Seizure-Induced Brain-Damaged Rats. *Electro-Magnetobiology* **1994**, *13*, 67–75. [[CrossRef](#)]
45. Baker-Price, L.; Persinger, M.A. Intermittent Burst-firing weak (1 microTesla) magnetic fields reduce psychometric depression in patients who sustained closed head injuries: A replication and electroencephalographic validation. *Percept. Mot. Ski.* **2003**, *96*, 965–974. [[CrossRef](#)] [[PubMed](#)]
46. Tsang, E.W.; Koren, S.A.; Persinger, M.A. Specific Patterns of Weak (1 microTesla) Transcerebral Complex Magnetic Fields Differentially Affect Depression, Fatigue, and Confusion in Normal Volunteers. *Electromagn. Biol. Med.* **2009**, *28*, 365–373. [[CrossRef](#)]
47. Thompson, M.E.; Zimmer, W.E.; Wear, L.B.; MacMillan, L.A.; Thompson, W.; Huttner, W.B.; Hidaka, H.; Scammell, J.G. Differential regulation of chromogranin B/secretogranin I and secretogranin II by forskolin in PC12 cells. *Mol. Brain Res.* **1992**, *12*, 195–202. [[CrossRef](#)]
48. Hussain, S.M.; Javorina, A.K.; Schrand, A.M.; Duhart, H.M.; Ali, S.F.; Schlager, J.J. The Interaction of Manganese Nanoparticles with PC-12 Cells Induces Dopamine Depletion. *Toxicol. Sci.* **2006**, *92*, 456–463. [[CrossRef](#)]
49. Pothos, E.; Przedborski, S.; Davila, V.; Schmitz, Y.; Sulzer, D. D2-Like Dopamine Autoreceptor Activation Reduces Quantal Size in PC12 Cells. *J. Neurosci.* **1998**, *18*, 5575–5585. [[CrossRef](#)]
50. Westerink, R.H.S.; Ewing, A.G. The PC12 cell as model for neurosecretion. *Acta Physiol.* **2008**, *192*, 273–285. [[CrossRef](#)]
51. Calon, F.; Tahar, A.H.; Blanchet, P.J.; Morissette, M.; Grondin, R.; Goulet, M.; Doucet, J.-P.; Robertson, G.S.; Nestler, E.; Di Paolo, T.; et al. Dopamine-receptor stimulation: Biobehavioral and biochemical consequences. *Trends Neurosci.* **2000**, *23*, S92–S100. [[CrossRef](#)]
52. Greengard, P.; Allen, P.B.; Nairn, A.C. Beyond the Dopamine Receptor: The DARPP-32/Protein Phosphatase-1 Cascade. *Neuron* **1999**, *23*, 435–447. [[CrossRef](#)]
53. Thompson, A.C.; Zapata, A.; Justice, J.B.; Vaughan, R.A.; Sharpe, L.G.; Shippenberg, T.S.  $\kappa$ -Opioid Receptor Activation Modifies Dopamine Uptake in the Nucleus Accumbens and Opposes the Effects of Cocaine. *J. Neurosci.* **2000**, *20*, 9333–9340. [[CrossRef](#)] [[PubMed](#)]
54. Fournier, N.M.; Mach, Q.H.; Whissell, P.D.; Persinger, M.A. Neurodevelopmental anomalies of the hippocampus in rats exposed to weak intensity complex magnetic fields throughout gestation. *Int. J. Dev. Neurosci.* **2012**, *30*, 427–433. [[CrossRef](#)] [[PubMed](#)]
55. Friedman, H.; Becker, R.O.; Bachman, C.H. Psychiatric Ward Behaviour and Geophysical Parameters. *Nat. Cell Biol.* **1965**, *205*, 1050–1052. [[CrossRef](#)]
56. Persinger, M.A. Wars and increased solar-geomagnetic activity: Aggression or change in intraspecies dominance? *Percept. Mot. Ski.* **1999**, *88* (Suppl. S3), 1351–1355. [[CrossRef](#)] [[PubMed](#)]